

CORRECTION

## Correction: A computational framework to study EGFR signaling distribution in egg chambers during dynamic interactions between soma and germline

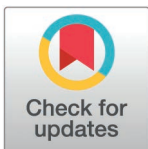
Nastassia Pouradier Duteil, Nicole T. Revaitis, Mathew G. Niepielko, Eric A. Klein, Nir Yakoby, Benedetto Piccoli

S1-S4 Figure images are omitted from the Supporting Information. It can be viewed below.

### Supporting information

**S1 Fig. Dynamic measurements of the egg chamber dimensions from S7 to S10A.** Data was collected at 6 consecutive time-points: 3hr (S7), 7.5hr (S8E), 10.5hr (S8L), 13.5hr (S9E), 16.5hr (S9L), 19.5hr (S10AE). A. Three measurements were taken in the AP direction: the total length of the egg chamber *LE*, the length of the oocyte *LO*, and the length of the follicle cells *LFC*. B. A cartoon schematic showing positions of measurements along the AP axis. C. Two measurements were taken in the DV direction: the egg chamber width *WE* and the oocyte width near the oocyte nucleus *WO*. D. A cartoon schematic showing positions of measurements along the DV axis. Note that the semi-axes of the prolate spheroid modeling the oocyte then correspond to half of the egg chamber length and width: and E. A cartoon schematic showing the different morphological transformations taken into account. The growth vector field, perpendicular to the egg chamber surface, is schematized by blue arrows. The follicle cells' shift, tangent to the egg chamber surface, is represented by green arrows. The oocyte nucleus' movement from (P) to (D), in the plane (xOz) is indicated by a grey arrow. (PDF)

**S2 Fig. Measurements of the source.** A. A cartoon depicting the vantage points from where source measurements were taken at the (i) Sagittal, denoted by red dotted line, (ii) Dorsal, denoted by yellow dotted line, and (iii) Anterior, denoted by blue dotted line. B. Immunohistochemistry stainings from vantage points of the egg chamber at S10A: (i) Sagittal (ii) Dorsal measurement from a ventral view (iii) Anterior boundary of oocyte. Corresponding table provides ratios of length of source compared to total length of domain (i.e. Sagittal (Sag), Dorsal (D), Anterior (A)) at S8 (n=6 D,A), S9 (n=8 for D, Sag,; n=10 A), and S10A (n=5 for D,Sag, n=9 for A). More precisely, Ratio (i) corresponds to the ratio of the dorsal length of the source with respect to the total (curved) length of the oocyte. Ratio (ii) corresponds to the ratio of the width of the source at the posterior of the nucleus with respect to the width of the



### OPEN ACCESS

**Citation:** Duteil NP, Revaitis NT, Niepielko MG, Klein EA, Yakoby N, Piccoli B (2026) Correction: A computational framework to study EGFR signaling distribution in egg chambers during dynamic interactions between soma and germline. PLoS Comput Biol 22(4): e1014155. <https://doi.org/10.1371/journal.pcbi.1014155>

**Published:** April 3, 2026

**Copyright:** © 2026 Duteil et al. This is an open access article distributed under the terms of the [Creative Commons Attribution License](https://creativecommons.org/licenses/by/4.0/), which permits unrestricted use, distribution, and reproduction in any medium, provided the original author and source are credited.

oocyte at the posterior of the nucleus. Ratio (iii) corresponds to the ratio between the curved width of the signal at the anterior of the nucleus and the half perimeter of the oocyte at the anterior of the nucleus. C. Representation of the numerical implementation of the source and table of experimental measurements of the source at specific stages. At S10A we show the current numerical implementation of the source compared to the source used in (Goentoro et al., 2006).  
(PDF)

**S3 Fig. A.** Parametrization of the prolate spheroid representing the egg-chamber at a given time  $t$  by  $(\eta, \theta) \in [0, \pi] \times [0, 2\pi]$ . The lengths of its semi-axes are  $LAP(t)$  (along the  $z$ -axis), and  $LDV(t)$  (along the  $x$  and  $y$ -axes). The posterior ( $P$ ) corresponds to  $\eta = 0$ , and the anterior ( $A$ ) to  $\eta = \pi$ . The dorsal side ( $D$ ) corresponds to  $\theta = 0$  and the ventral side ( $V$ ) to  $\theta = \pi$ . The oocyte nucleus, represented by the gray circle, migrates from the posterior to the dorsal anterior of the spheroid. B-E. Construction of the cubed spheroidal mesh. The cubed spheroidal mesh is obtained by a two-step transformation, from the cube  $Ca$  to the sphere  $SAP$ , and from the sphere  $SAP$  to the spheroid  $P$ . Consider the sphere of radius  $SAP$  centered at 0 and let  $Ca$  be its inscribed cube of side, also centered at 0. Each side of  $Ca$  is discretized by a regular orthonormal mesh (D). Then the cubed spherical mesh of  $SAP$  is obtained by taking the radial projection of the mesh of  $Ca$  onto  $SAP$  (D and B): each vertex  $PC(xc, yc, zc) \in Ca$  of the mesh is projected radially onto  $SAP$ , giving the point  $PS(xS, yS, zS) \in SAP$ . By this transformation, the sphere  $SAP$  is meshed by the cubed sphere projection. Secondly, each vertex  $PS \in SAP$  of the cubed spherical mesh is projected onto the prolate spheroid  $P$ , orthogonally to the  $z$ -axis (C). This transformation defines the cubed spheroidal mesh (E). F-G. Division of the prolate spheroid  $P$  into subdomains. From the cubed spheroid mesh construction, each quarter spheroid is divided into 4 subdomains, corresponding to four sides of the cube. In S3 Fig F, we represent the quarter spheroid contained in the region  $\{(x, y, z) \in \mathbb{R}^3, y \geq 0, z \geq 0\}$ . It is divided into the subdomains  $S0$  (covering the posterior pole),  $S1$  (dorsal region),  $S2$  (lateral region) and  $S3$  (ventral region). S3 Fig G shows the boundary conditions implemented at the subdomain interfaces. Dotted lines represent matching boundary conditions, whereas continuous lines indicate Neumann boundary conditions (due to the symmetry property). The mesh for the region  $\{(x, y, z) \in \mathbb{R}^3, y \leq 0, z \geq 0\}$  is obtained by symmetry with respect to the plane  $XZ$ , and the meshes for the regions  $\{(x, y, z) \in \mathbb{R}^3, y \geq 0, z \leq 0\}$  and  $\{(x, y, z) \in \mathbb{R}^3, y \leq 0, z \leq 0\}$  are then obtained by symmetry with respect to the plane  $XY$ . In fact, the problem is symmetric with respect to the plane  $(XZ)$ , so the solution is computed only for the semi-spheroid  $y \geq 0$ .  
(PDF)

**S4 Fig. Intensity plots of dpERK and GRK at stages 8 through 10A of oogenesis.** A. Intensity profiles of GRK for varying GRK copy numbers at 2x (OreR), 4x, and 1x along the AP (top row) and DV (bottom row). B. Intensity profiles of dpERK for varying GRK copy numbers at 2x (OreR), 4x, and 1x along the AP (top row) and DV (bottom row). C. Intensity profiles of GRK for three genetic backgrounds: wild-type (OreR), STY- RNAi, and EGFR-RNAi along the AP (top row) and DV (bottom row).

D. Intensity profiles of dpERK for three genetic backgrounds: wild-type (OreR), STY- RNAi, and EGFR-RNAi along the AP (top row) and DV (bottom row).

(PDF)

## Reference

1. Duteil NP, Revaitis NT, Niepielko MG, Klein EA, Yakoby N, Piccoli B. A computational framework to study EGFR signaling distribution in egg chambers during dynamic interactions between soma and germline. PLoS Comput Biol. 2025;21(12):e1013802. <https://doi.org/10.1371/journal.pcbi.1013802> PMID: [41460945](https://pubmed.ncbi.nlm.nih.gov/41460945/)